

Antropopresja i zmiany pokrycia terenu w obszarach chronionych

Sebastian Aleksandrowicz (CBK PAN)





Obszary chronione



Liczba obszarów chronionych:
Świat: 276 864

Polska: 3109

Parki Narodowe: 23

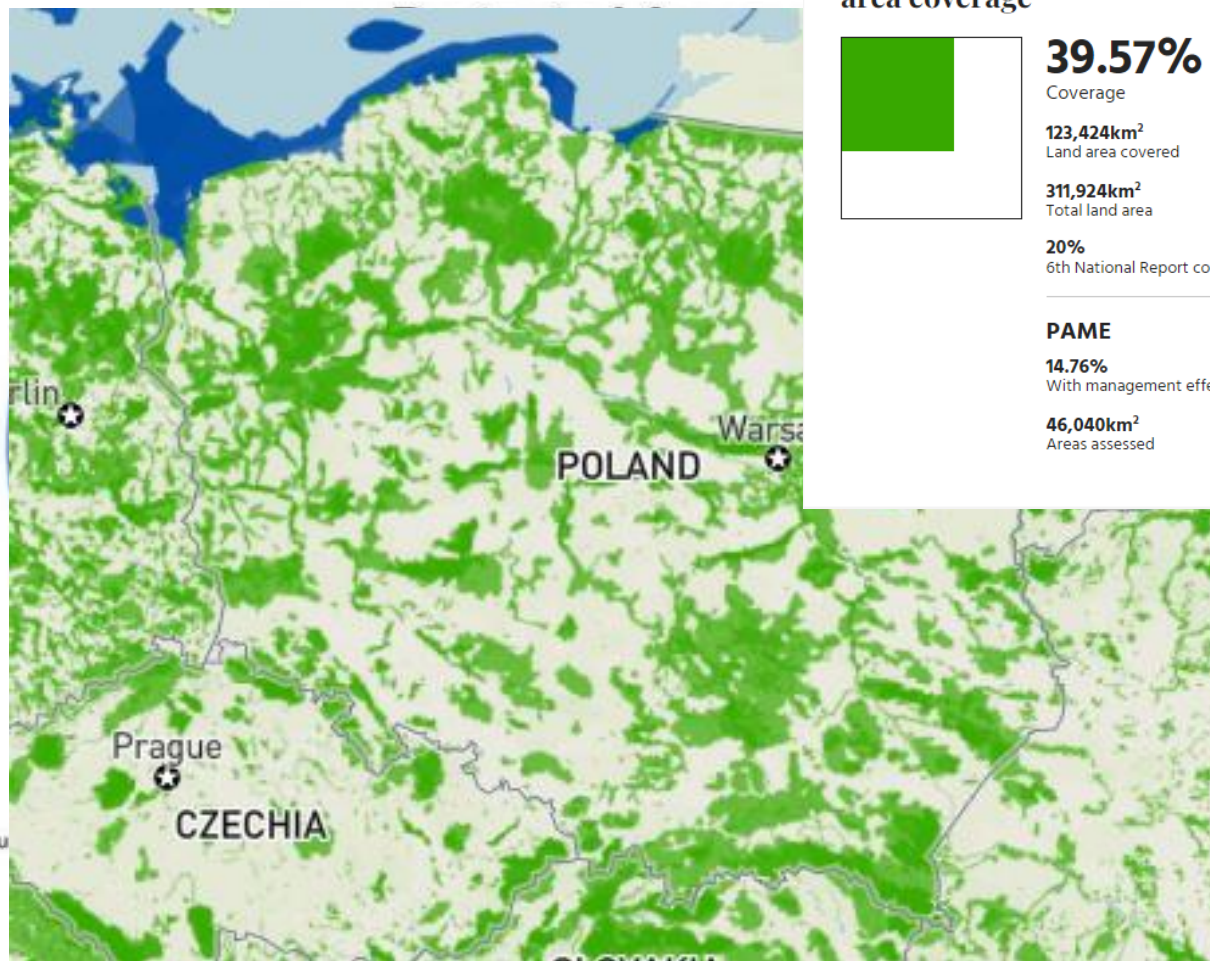
Rezerwaty przyrody: 1499

Parki krajobrazowe: 124

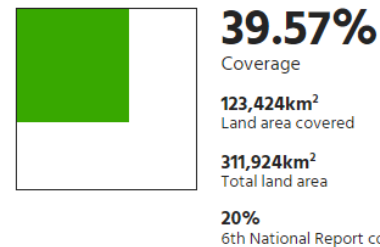
Obszary chronionego krajobrazu: 407

Obszary Natura 2000: 994

Źródło danych: crfop.gdos.gov.pl



Terrestrial and inland waters protected area coverage

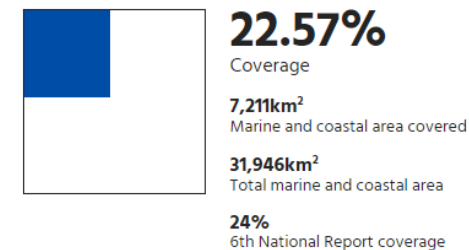


PAME

14.76%
With management effectiveness evaluations

46,040km²
Areas assessed

Marine protected area Coverage



PAME

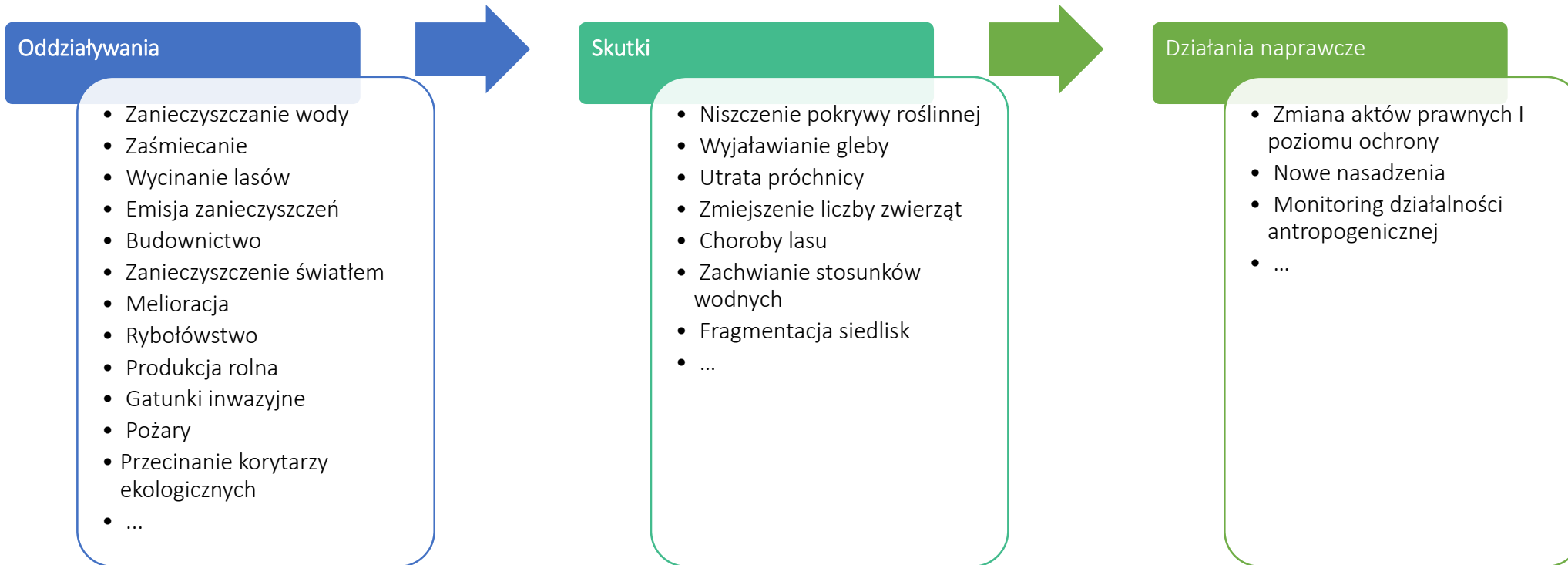
19.9%
With management effectiveness evaluations

6,356km²
Areas assessed

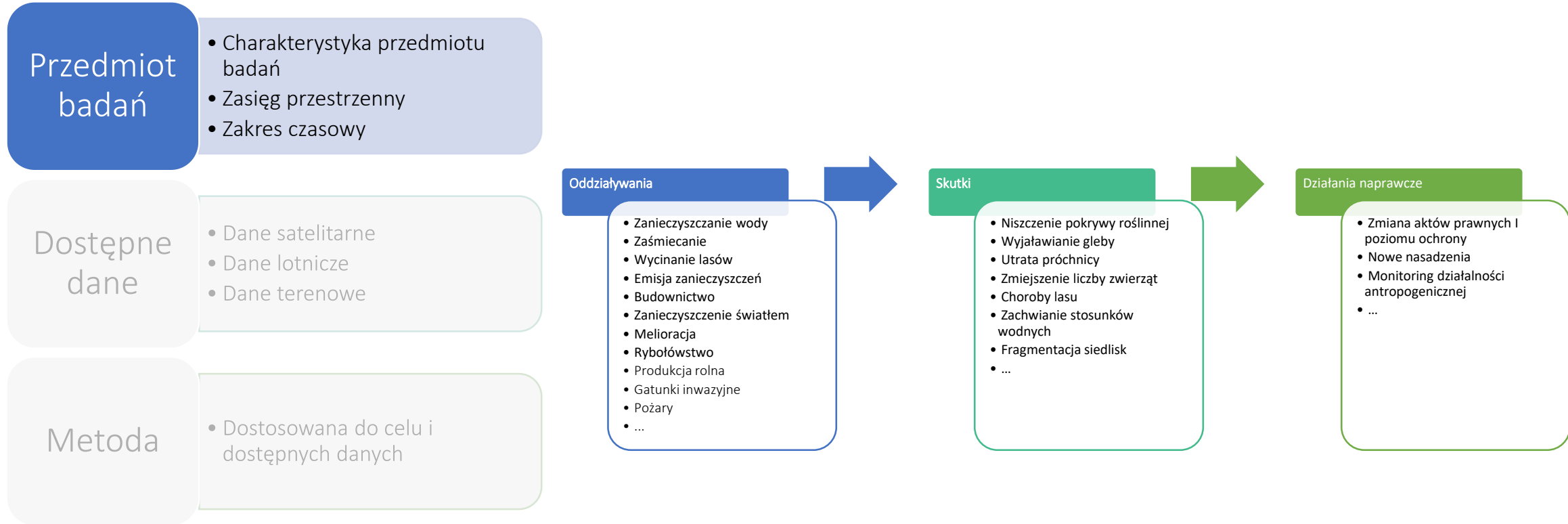
Źródło: <https://www.protectedplanet.net/>



Antropopresja a badania satelitarne



Jak badać antropopresję z poziomu satelity?



Jak badać antropopresję z poziomu satelity?

Przedmiot badań

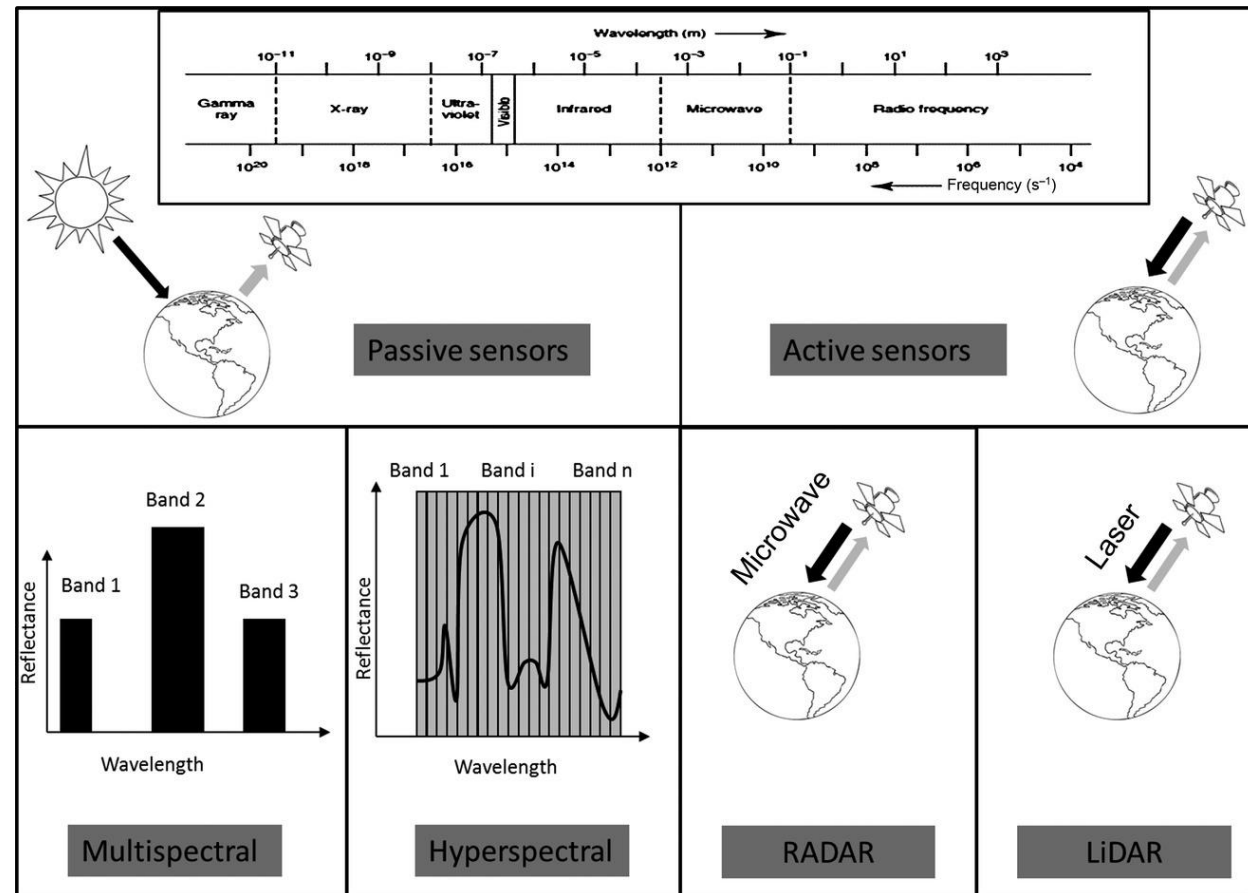
- Charakterystyka przedmiotu badań
- Zasięg przestrzenny
- Zakres czasowy

Dostępne dane

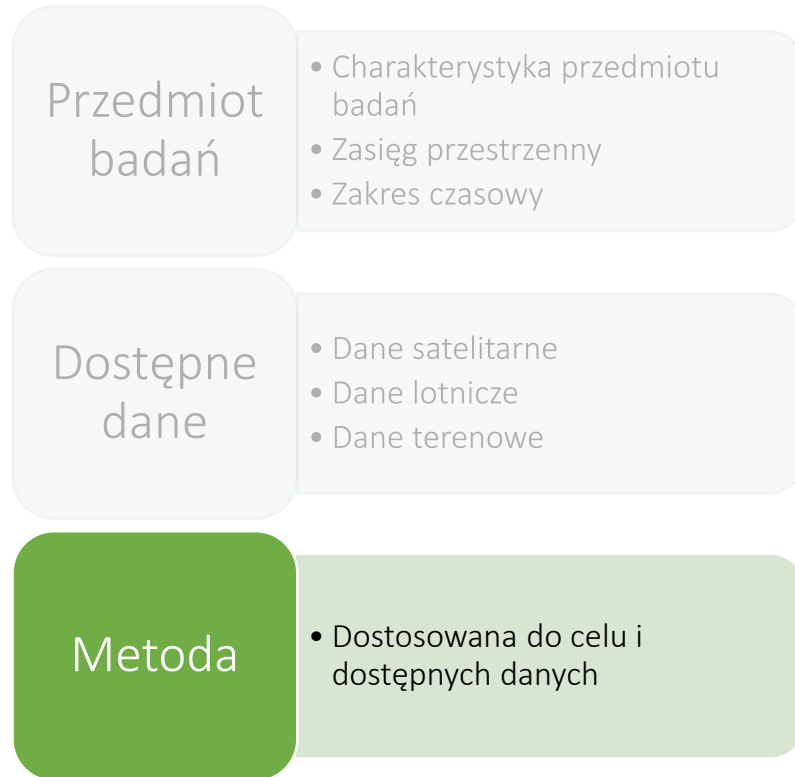
- Dane satelitarne
- Dane lotnicze
- Dane terenowe

Metoda

- Dostosowana do celu i dostępnych danych



Jak badać antropopresję z poziomu satelity?





Analizy wizualne

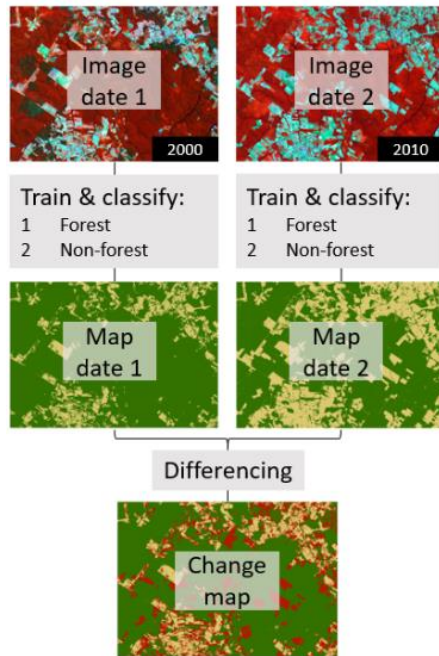
Źródło: <https://pubs.usgs.gov/of/2004/1451/brown/>



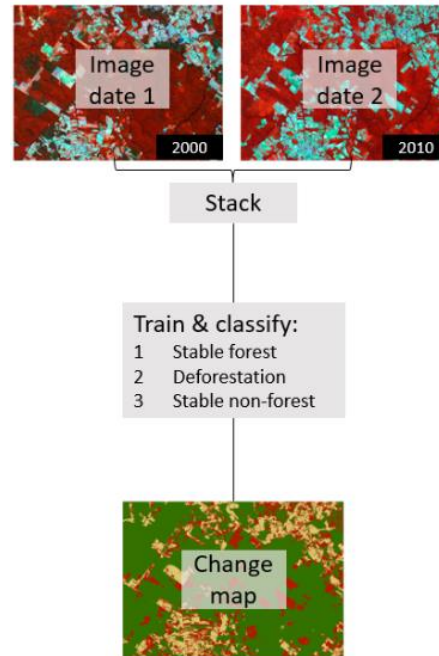
Oparta na algebrze

Porównanie klasyfikacji pokrycia terenu

Post-classification change detection



Multi-temporal change classification



$$T_{\Delta} = T_2 - T_1$$

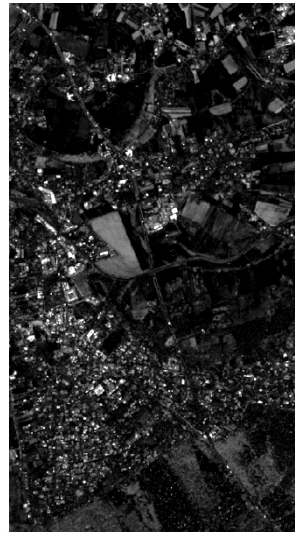
$$NDVI_{\Delta} = NDVI_2 - NDVI_1 \quad NDVI = \frac{(NIR - R)}{(NIR + R)}$$

$$NBR_{\Delta} = NBR_2 - NBR_1 \quad NBR = \frac{(NIR - SWIR)}{(NIR + SWIR)}$$

... i ponad 240 innych indeksów dla Sentinela-2

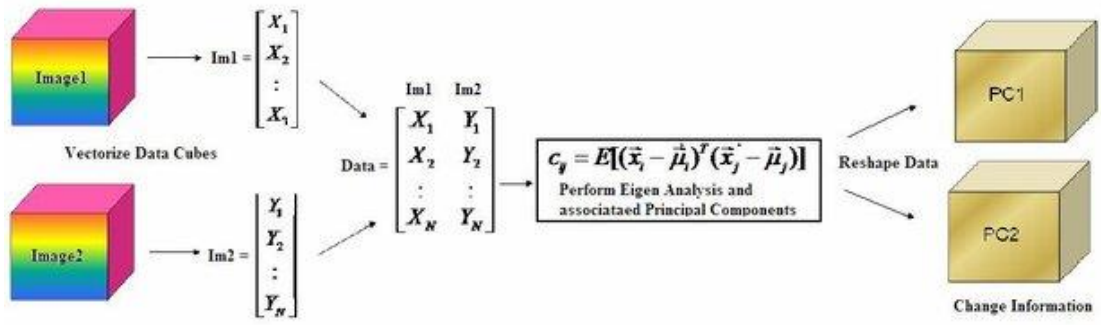


$$\begin{bmatrix} X \\ Y \end{bmatrix} \rightarrow \begin{bmatrix} a_p^T X - b_p^T Y \\ \vdots \\ a_1^T X - b_1^T Y \end{bmatrix}$$



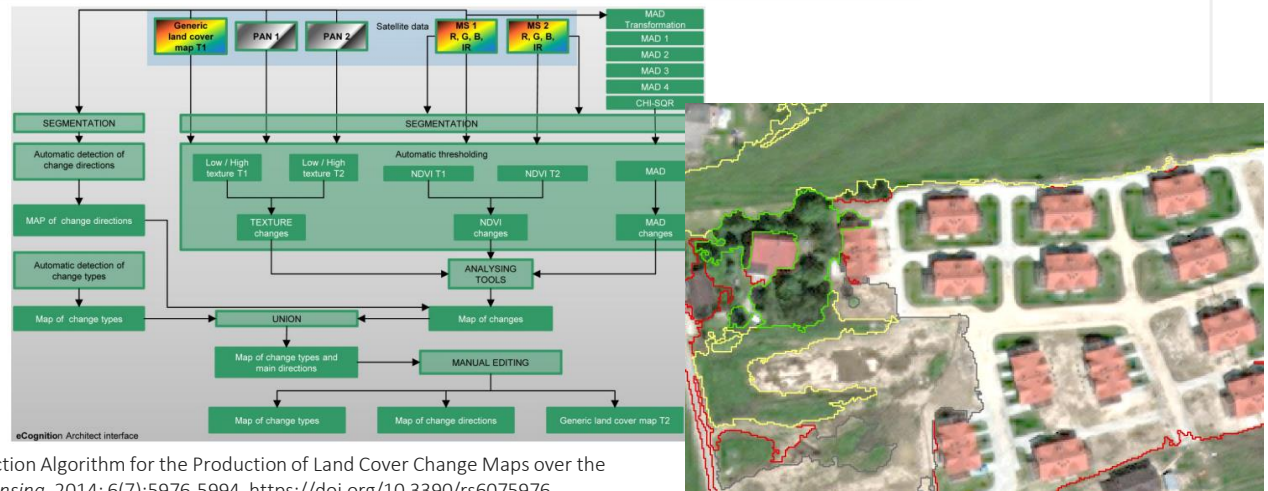
Transformacje
(PCA, TC, MAD)

- Multivariate Alteration Detection
- Tasseled Cap
- Principal Component Analysis



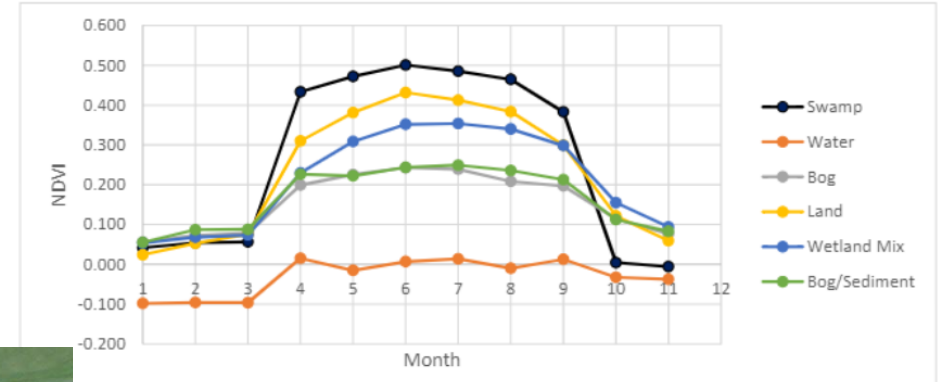
Źródło: Vongsy, et.al. (2007). Change detection for hyperspectral imagery. Proceedings of SPIE - The International Society for Optical Engineering. 10.1117/12.723161.

Metody obiektowe



Aleksandrowicz S, et. al. Change Detection Algorithm for the Production of Land Cover Change Maps over the European Union Countries. *Remote Sensing*. 2014; 6(7):5976-5994. <https://doi.org/10.3390/rs6075976>

Analiza serii czasowych



Kaplan, Gordana & Avdan, Ugur. (2018). Monthly Analysis of Wetlands Dynamics Using Remote Sensing Data. *International Journal of Geo-Information*. 7. 1-20. 10.3390/ijgi7100411.



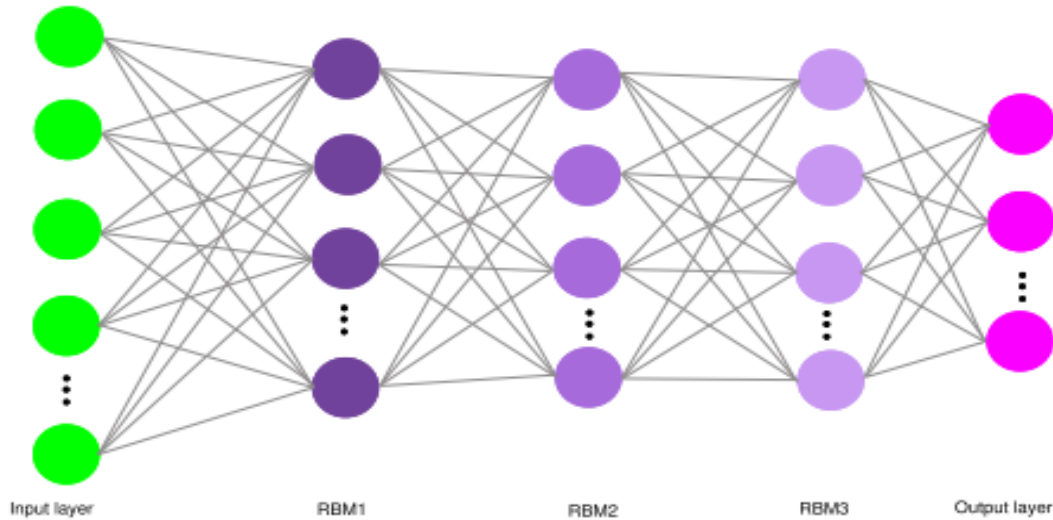


Metody wykorzystujące uczenie maszynowe:

- Random Forest
- Support Vector Machines
- Decision Trees
- Boosting



Deep learning



Author	Year	Techniques	Mode	Advantage	Disadvantage
Peng et al. [157]	2019	U-Net++	Supervised	End-to-end	Require huge training sample
Fang et al. [158]	2019	DLSF	Supervised	High detection performance	Not focus on spectral information changes.
Chen et al. [159]	2019	SiamCRNN	Supervised	High performance	Large number of labeled sample
Jing, R et al. [160]	2020	TriSiamese LSTM	Supervised	Improved accuracy	Computational complexity
Javed et al. [161]	2020	D-S theory	Unsupervised	Low false alarm	Miss detection of building changes
Correa et al. [162]	2018	Tree of radiometric change	Unsupervised	Good performance	Lot of training sample
Saha et al. [163]	2019	Multi-layered CNN	Unsupervised	Reduce dependence on changing samples	Needs a large number of pixel-level samples.
Zhao et al. [164]	2020	AG-GAAN	Unsupervised	Improve the detection accuracy	Model is greatly challenged by the hazardous environments
Papadomanolaki et al. [167]	2021	LU-Net	Unsupervised	Novel method	Low performance
Saha et al. [165]	2020	GCN	Semi-supervised	Eliminates many redundant features	Time consuming
Pang et al. [157]	2021	SCA-CDNet	Pretrained	Improve accuracy	Insufficient for some practical applications
Ji et al. [168]	2019	Mask R-CNN, CNN	Self-trained	Reduce the demand of training samples	Time complexity

Zestawienie metod detekcji zmian opartych na metodach deep learningu wykorzystujących dane VHR (źródło: Shafique A, Cao G, Khan Z, Asad M, Aslam M. Deep Learning-Based Change Detection in Remote Sensing Images: A Review. Remote Sensing. 2022; 14(4):871. <https://doi.org/10.3390/rs14040871>)



Wylesienia

Global Land Analysis & Discovery

Search places

Layers Mapa Sateilita

Global Forest Change

Published by Hansen, Potapov, Moore, Hancher et al.

University of Maryland
Department of Geographical Sciences

Results from time-series analysis of Landsat images characterizing forest extent and change.

Trees are defined as vegetation taller than 5m in height and are expressed as a percentage per output grid cell as '2000 Percent Tree Cover'. 'Forest Cover Loss' is defined as a stand-replacement disturbance, or a change from a forest to non-forest state, during the period 2000-2012. 'Forest Cover Gain' is defined as the inverse of loss, or a non-forest to forest change entirely within the period 2000-2012. 'Forest Loss Year' is a disaggregation of total Forest Loss to annual time scales.

Reference 2000 and 2022 imagery are median observations from a set of quality assessment-passed growing season observations.

To share location copy URL.

Download the data.

Data Products

Forest Loss Year (2022 Highlight)

- 2022
- 2021
- 2020
- No loss
- Water or no data

Other Data Layers

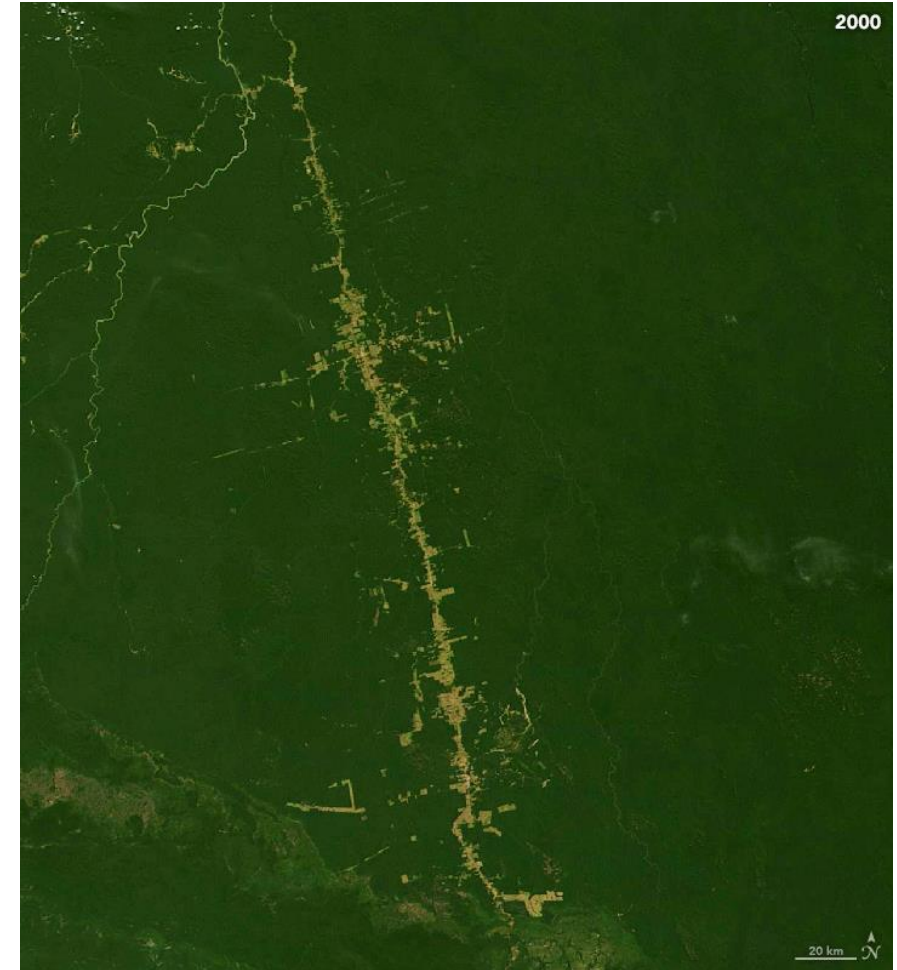
2000 Percent Tree Cover

Background Imagery

Year 2000 Bands 5/3/4

Example Locations

Forestry and Tornado in Alabama





Oddziaływanie

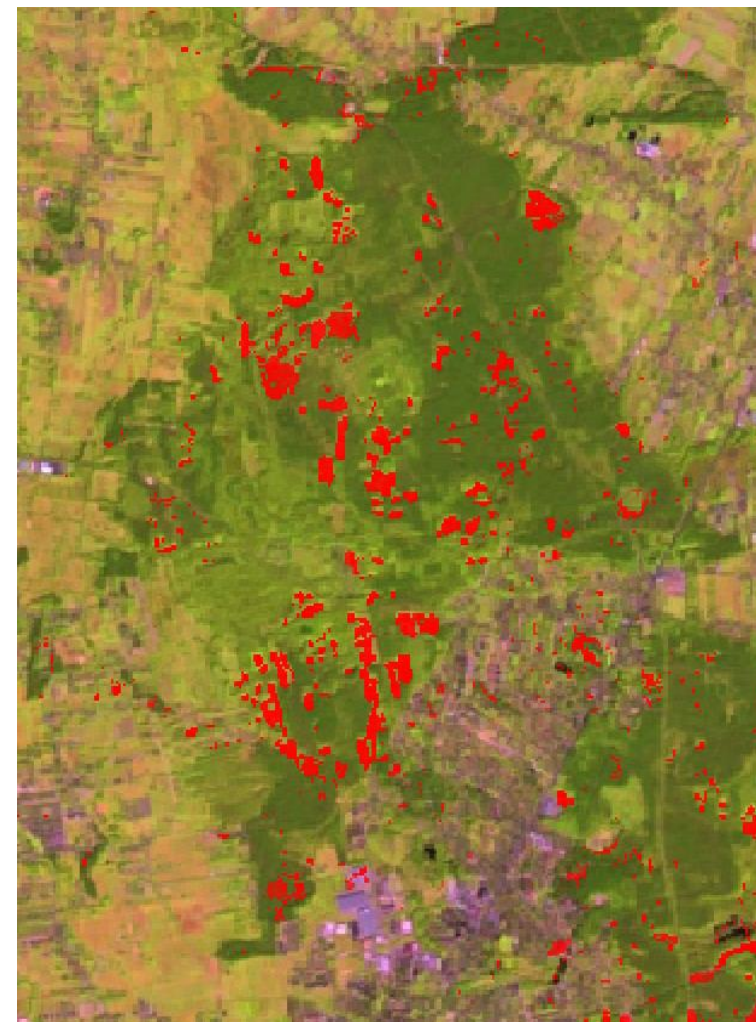
Wylesienia



2000



2022

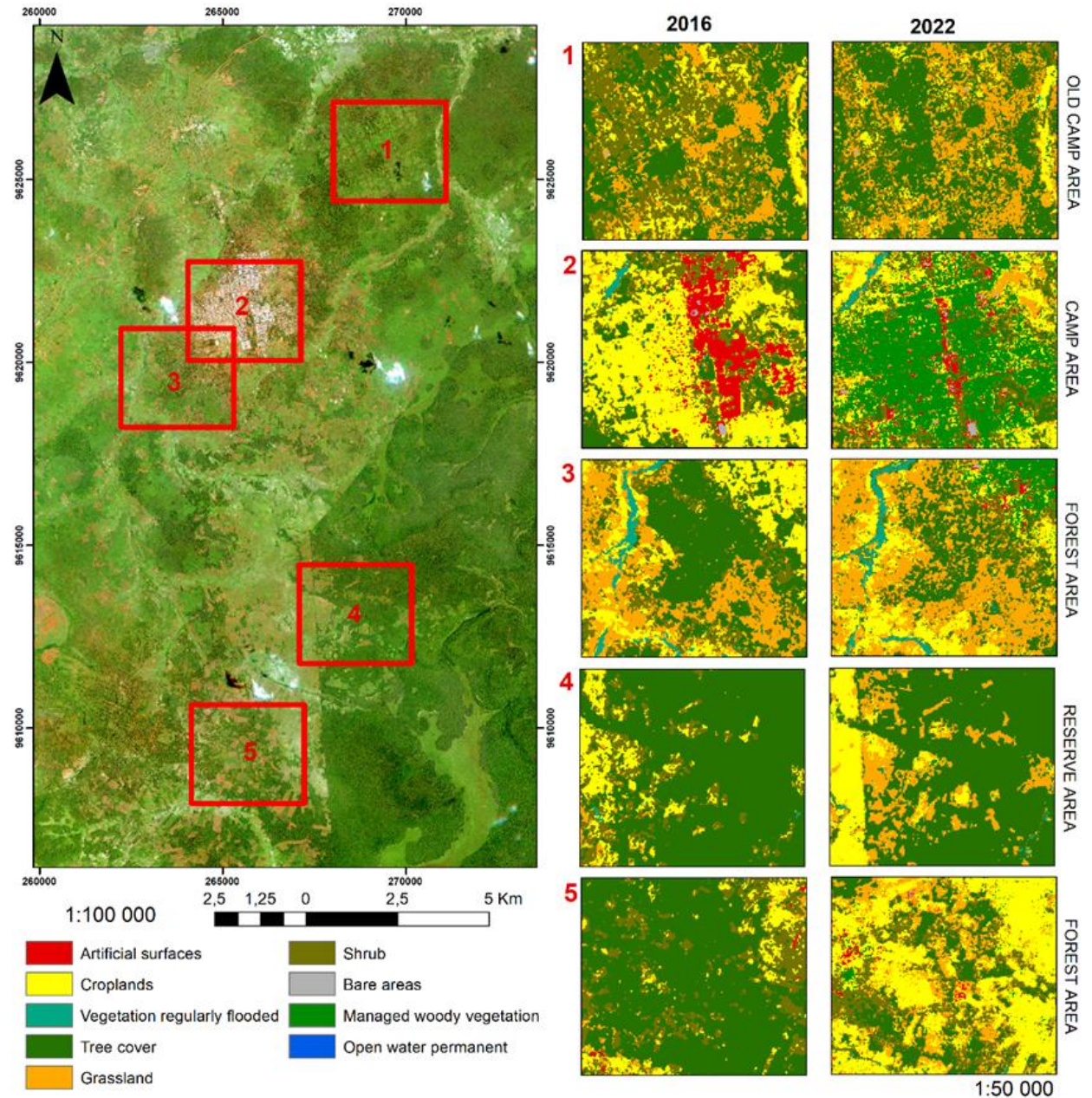


Wynik detekcji zmian

Wylesienia

Wpływ powstania obozu dla uchodźców w pobliżu rezerwatu Moyowosi Geme Reserve (Tanzania)

- Odbudowa szaty roślinnej po poprzednim obozie
- Powstanie, rozwój i zamknięcie nowego obozu
- Intensyfikacja rolnictwa i wylesienia



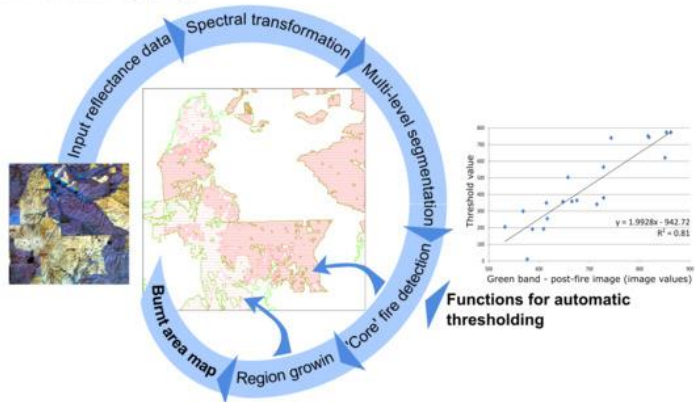
Požary



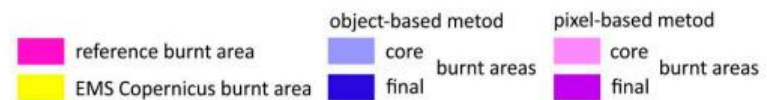
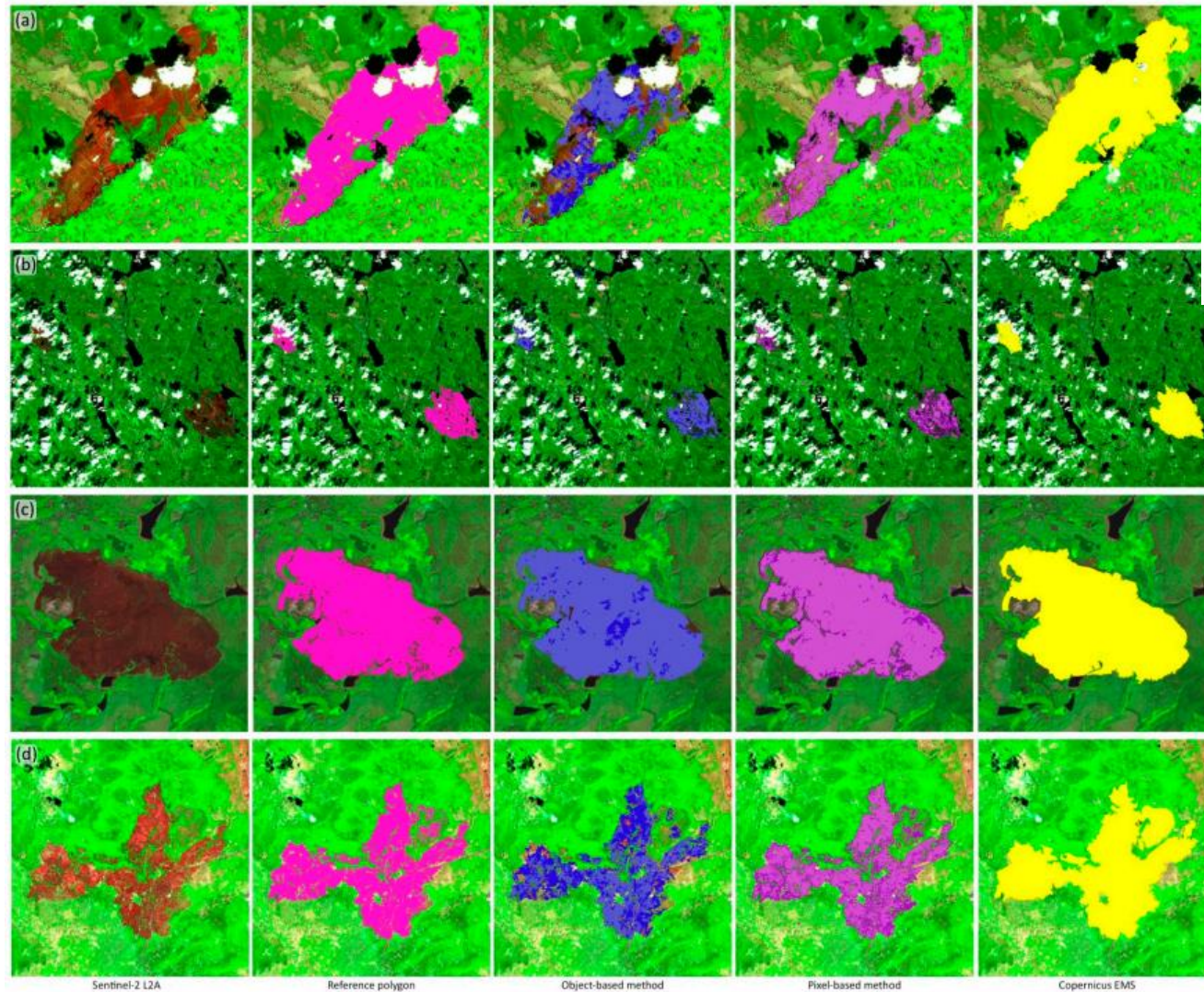
Oddziaływania

Skutki

Burnt area mapping



Woźniak E, Aleksandrowicz S. Self-Adjusting Thresholding for Burnt Area Detection Based on Optical Images. *Remote Sensing*. 2019; 11(22):2669. <https://doi.org/10.3390/rs11222669>

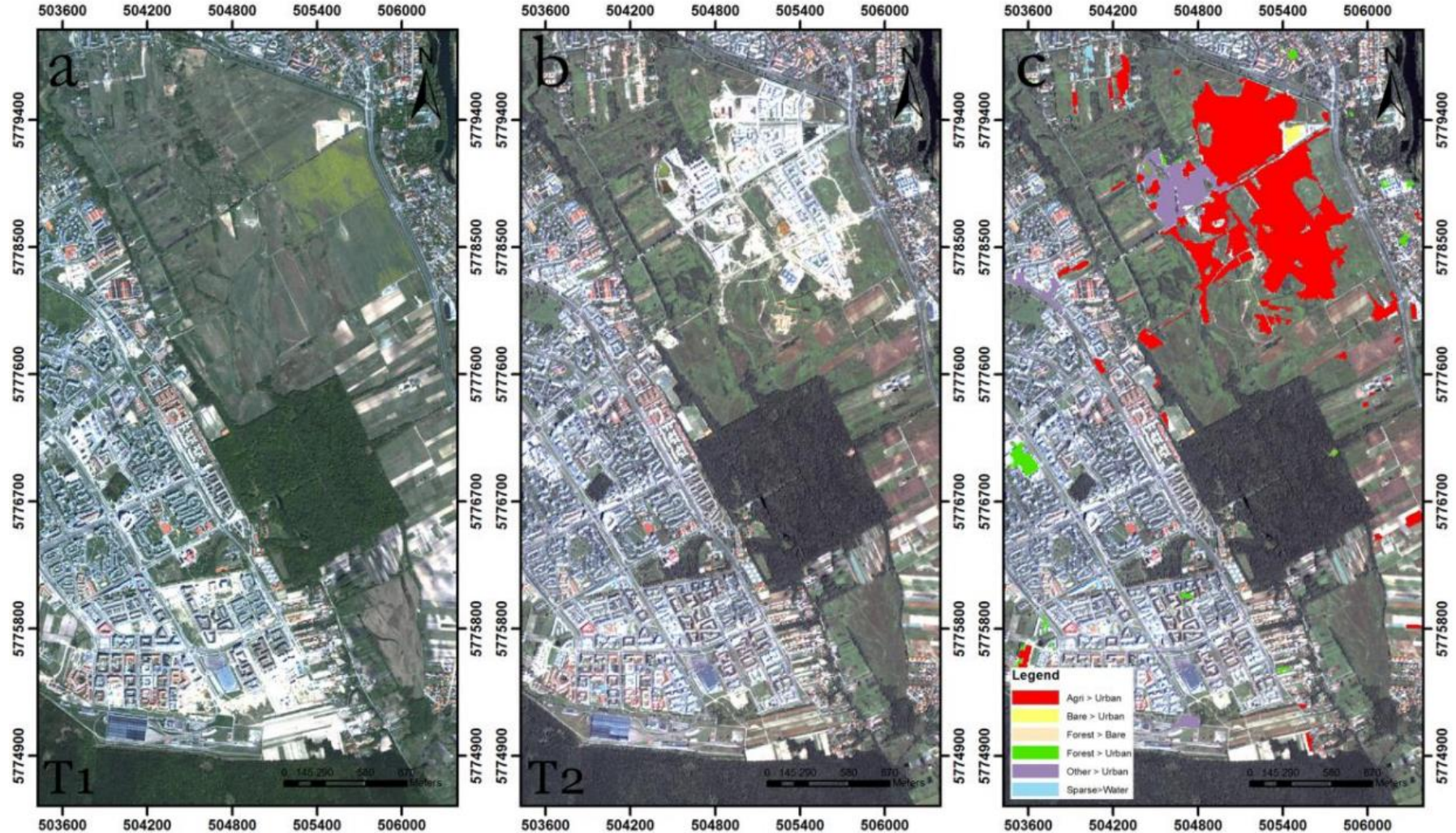


Detekcja zmian na zdjęciach bardzo wysokiej rozdzielczości z wykorzystaniem transformacji MAD oraz metod obiektowego przetwarzania obrazu.

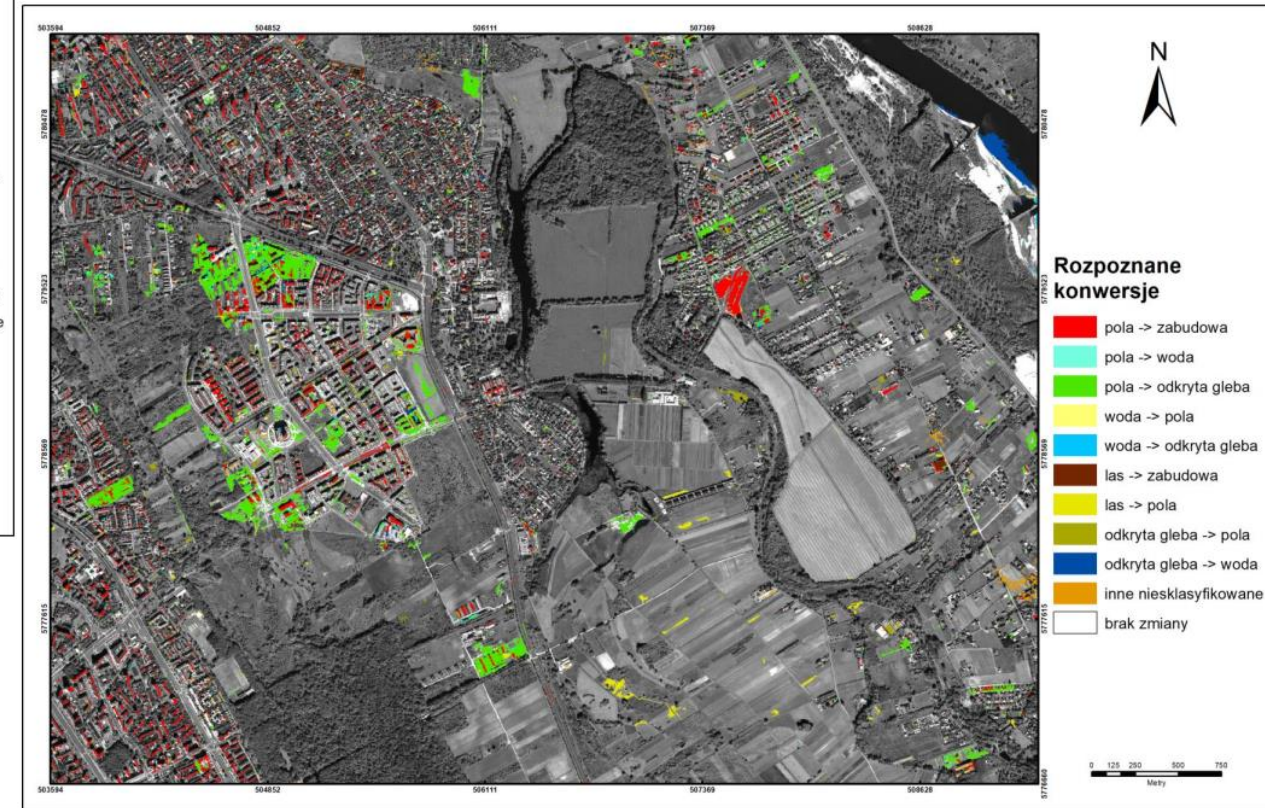
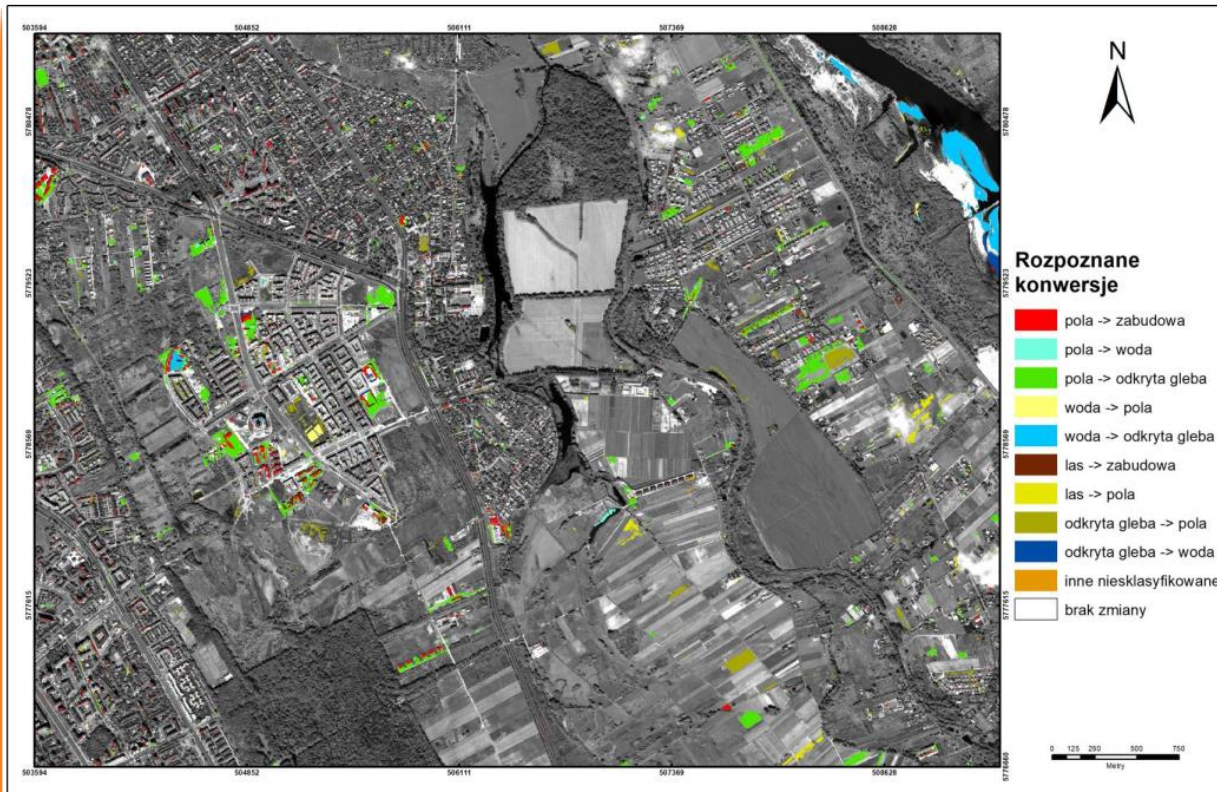
Zdjęcia Ikonos:

T1 – 2002 r.

T2 – 2008 r.



Urbanizacja



Wynik detekcji zmian na parach zdjęć WorldView-2 pozyskanych w 2010, 2013 i 2016 roku dla fragmentu m. st. Warszawy

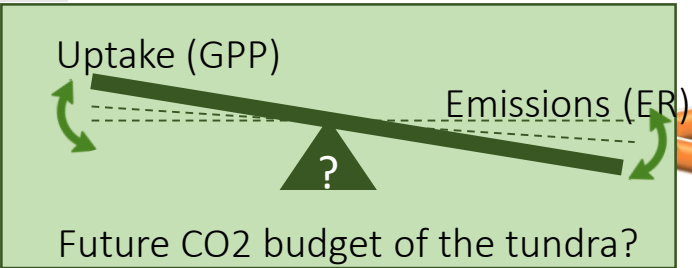


Skutki

Modelowanie Produkcji Pierwotnej brutto (Gross Primary Productivity - GPP)

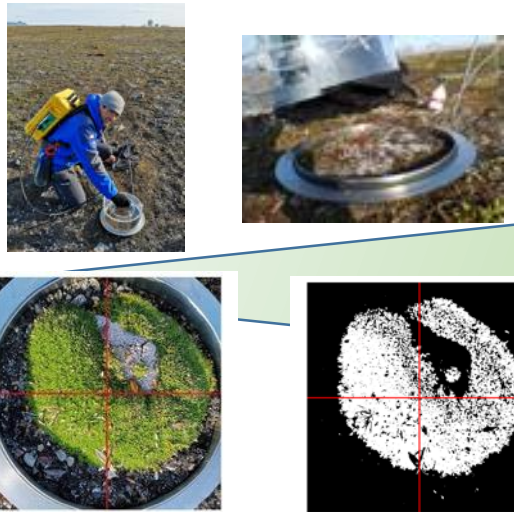
Arctic tundra: Svalbard Critical Zone Observatory

Alpine tundra: Nivolet Critical Zone Observatory



RQ: what are the drivers of CO₂ fluxes?

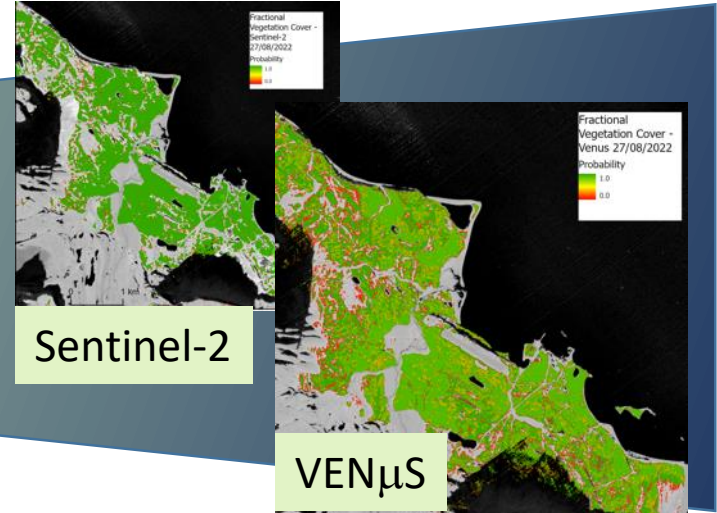
Site scale: *In-situ* flux chambers



Ecosystem scale: Eddy Covariance



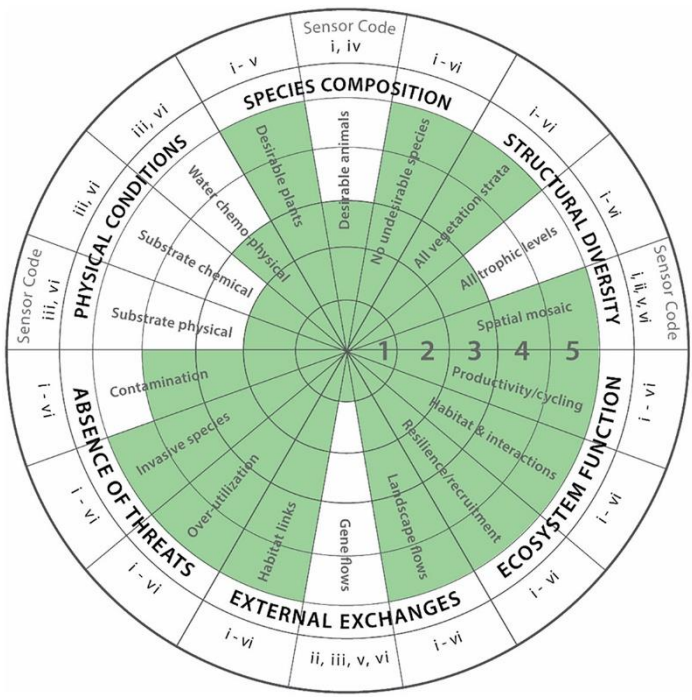
Regional scale: remote sensing



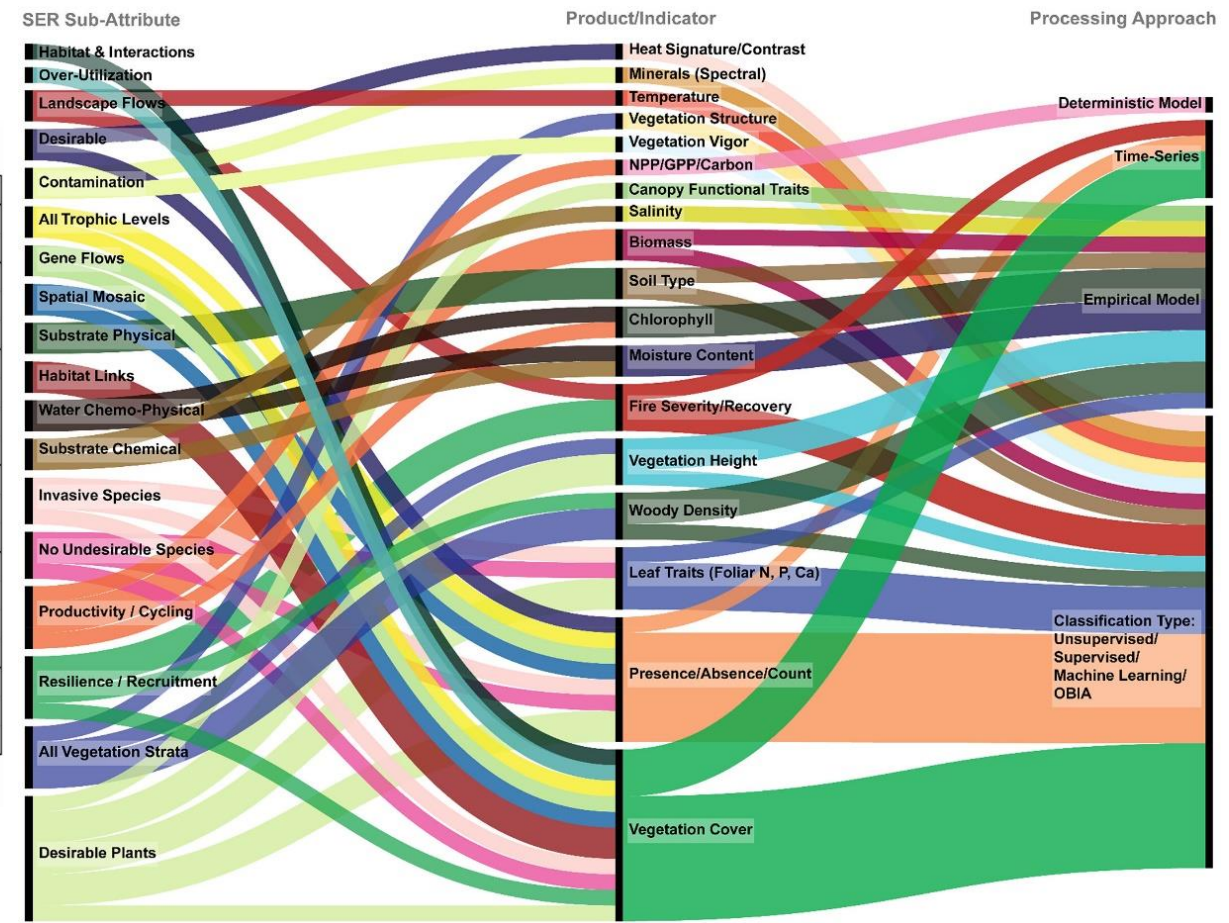
Źródło: M.S. Giamberini (1), S. Aleksandrowicz (2), F. Avogadro (1), I. Baneschi (1), A. Baronetti (1), A. Karnieli (3), M. Magnani (1), S. Marta (1), A. Monteiro (1, 4), N. Panov (3), A. Parisi (1), M. Salvoldi (3), S. Vicario (5), G. Vivaldo (1), E. Woźniak (2), A. Provenzale (1) Measuring and Modelling Gross Primary Productivity in Alpine and Arctic Tundra: from Point to Landscape Scale Using Satellite Data



Monitoring działań naprawczych



Sensor Code	Sensor	Platforms
i	Red Green Blue (RGB)	a Drone b Aerial
ii	Multispectral	a Drone b Aerial c EO (High, Med, Low)
iii	Hyperspectral	a Handheld b Drone c Aerial d EO (High, Med, Low)
iv	Thermal	a Drone b Aerial c EO (High, Med, Low)
v	LIDAR	a Terrestrial laser Scanner b Drone c Aerial d EO (High, Med, Low)
vi	Imaging RADAR/SAR	a Drone b Aerial c EO (High, Med, Low)





Strengths Weaknesses Opportunities Threats

